*energies*

MDPI

*Article*

# Experimental Investigation on Crack Development Characteristics in Shallow Coal Seam Mining in China

**Qingxiang Huang [1,2,*], Yanpeng He [1,2,*] and Jian Cao [1,2]**

1 School of Energy Engineering, Xi'an University of Science and Technology, Xi'an 710054, China; caoj@stu.xust.edu.cn
2 Key Laboratory of Western Mine Exploitation and Hazard Prevention with Ministry of Education, Xi'an University of Science and Technology, Xi'an 710054, China
* Correspondence: huangqx@xust.sn.cn (Q.H.); heyp@stu.xust.edu.cn (Y.H.); Tel.: +86-130-8895-7981 (Q.H.); +86-180-9182-7090 (Y.H.)

Received: 27 February 2019; Accepted: 31 March 2019; Published: 4 April 2019

**Abstract:** The development of cracks in mining is the scientific basis for the safety and environmental exploitation of shallow multiple-seam. According to the "thickness of coal seam, interactive distance, and buried depth," four mining coal mines are selected in Shen Fu-Dong Sheng coalfield (SFDSC). To research the mining conditions of shallow coal seam under different base-load ratio mining conditions and different working faces by the physics simulation and in-sit measurement, the key roof caves are sketched by different colors. This study shows that the typical shallow coal seams in the thin overlying bedrock and thick loose sand layer (LSL) as well as the development of the setup entry cracks (SEC) is dominated by LSL arch damage. The surface cracks are almost directly above the setup entry. The flat seam mining and the SEC development is dominated by parabolic type. The surface cracks are located inside the setup entry. With the mining height increased typically in a shallow coal seam, the rate of crack development and the extent of damaged area increased significantly. The SEC and boundary cracks are fixed. The dynamic periodic cracks (DPC) show the ability of the strata to self-repair. During the multiple-seam mining, the above three kinds of cracks have the phenomenon of activation and development. Through the reasonable coal pillar distance arrangement, the development of boundary cracks can be effectively controlled and the relatively uniform surface settlement and crack closure can be achieved. The purpose of reducing damage mining can also be achieved. Furthermore, it provides scientific support for the green mining in the shallow coal seam.

**Keywords:** shallow coal seam; multiple-seam mining; crack growth; sketch drawing; coal pillar distance; reduce damage mining; green mining

## 1. Introduction

The Jurassic coalfield is located in northern SFDSC. The seams are generally characterized by shallow depth, is nearly horizontal, and has three to four workable coal seams. The interactive distance is about 20 to 40 m (Figure 1), so it belongs to the multiple-seam mining. With the continuous consumption of mineral resources, multiple-seam mining has become an inevitable trend. The realization of environmentally-friendly multiple-seam mining is a major topic in science mining in the shallow coal seam [1–4].

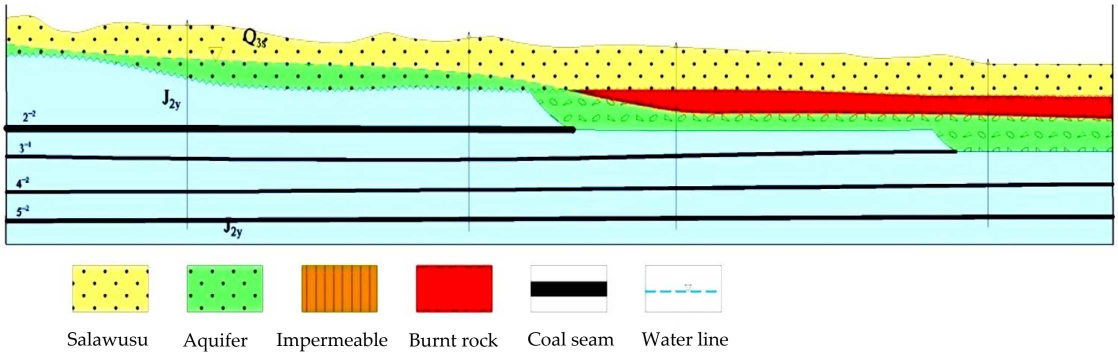


**Figure 1.** Sectional view of workable coal seams from Zhangjiamao Coal Mine in SFDFC, China.

In recent years, domestic scholars have carried out extensive research on surface subsidence and ground cracks in shallow coal seam, and have become one of the new hot topics. Huang et al. [5,6] found that the load transfer effect under the thick LSL mining and the law of the key block load transfer is given. The stability of the water resistant key strata in strip filling is an effective way to protect water mining. The height formula for the "upward crack" and "downward crack" of the strip filling water retention is given [7,8]. Liu [9,10] analyzed the law of the dynamic development of mining ground cracks in shallow coal seam, and proposed corresponding treatment techniques. Hu et al. [11,12] conducted in-depth research on the distribution characteristics and development of subsidence ground cracks in shallow coal seam. Hu et al. pointed out the impact of mining on the surface environment is mainly subsided ground cracks and the edge cracks are the focus of restoration.

Fan [13,14] used remote sensing technology to study the distribution of ground cracks in the Yushenfu mining area and found the high-strength mining areas in the loess gully area have dense ground cracks and serious surface damage. Chen [15,16] studied the distribution characteristics and formation mechanism of surface cracks in the Shendong mining area, pointed out that surface dynamic tensile cracks appeared periodically with the advancement of the working surface, and stepped cracks appeared near the boundary of the working surface. The overburden stress distribution map is presented. Yu et al. [17–19] researched on mining cracks under different mining conditions. Peng et al. [20] conducted a large-scale three-dimensional physical similarity simulation experiment in order to explore the development mechanism of Xi'an ground fissure, which provided some enlightening significance for the mining engineering physical similarity simulation experiment to study mining cracks. Mao et al. [21] proposed the integrated management of coal mine spatial information, based on the "temporal" characteristics of coal mine data, expounding the importance of spatio-temporal synergy between underground and ground, and providing technical support for the dynamic study of surface cracks. Xu et al. [22] studied the caving pattern of overlying strata and determined the calculation method of fracture pathway parameters due to roof caving induced by coal mining. Zhang et al. [23] applied the geophysical-chemical properties of radon in mining engineering, and the field-measured results are good.

However, most of the above academics are based on the actual measurement and numerical simulation analysis of the shallow coal seam in the thick rock and loose layer. The study on the shallow buried thin rock and thick loose layer has not deepened. The secondary development mechanism of surface cracks needs to be improved in shallow multiple-seam mining.

Based on a large number of physical similarity simulation experiments, the law of crack evolution in shallow single coal seam under different base-load ratio mining conditions is investigated. Study on the secondary development law of cracks in multiple-seam mining, and the cracking field of repeated mining overburden is revealed. In addition, the coupling mechanism of surface cracks provides a scientific basis for the safe and environmentally-friendly mining in shallow coal seam.

## 2. Physical Simulation Design and Methods

### *2.1. Experimental Design*

Huang [24] proposed a scientific definition of typical shallow coal seam and near shallow coal seam. Characteristics of the typical shallow coal seam, the thin overlying bedrock and thick LSL, with the single key stratum, the roof is easily broken and the step is sinking. However, the near shallow coal seam has the thick overlying bedrock and thin LSL, with double or three key stratums. According to the ratio of thickness of coal seam and interactive distance, and whether the inter-burden contains key stratum, the shallow multiple-seam is divided two types including utmost closely spaced multiple-seam, and closely spaced multiple-seam. Combined with a large number of physical simulation in shallow coal seam and shallow multiple-seam mining, analyzed the physical simulation of the crack evolution law (PSCEL) of shallow coal seam mining.

Physical simulation experiments used similar principles to determine similarity constants, in order to simulate actual mining formations. Based on "thickness of coal seam, interactive distance, and buried depth," four coal mines are selected in SFDSC, and the parameters of coal and its roof and floor are listed in Table 1. Those values in Table 1 were obtained from the experimental determination or from the references [1,7,8].

**Table 1.** The parameters of coal and its roof and floor of four coalmines.

| Coal Mine (Working Face) | Lithology | Thickness (m) | Bulk Density (kg/m$^3$) | Young's Modulus (GPa) | Compressive Strength (MPa) | Cohesion (MPa) | Poisson's Ratio |
|---|---|---|---|---|---|---|---|
| Daliuta (1203) | Sand layer | 45.0 | 2.25 | 0.18 | 7 | 0.02 | 0.4 |
| | Fine sandstone | 13.0 | 2.4 | 16.24 | 48 | 7.4 | 0.21 |
| | Siltstone | 6.0 | 2.4 | 9.83 | 36 | 7.2 | 0.14 |
| | No. 1-2 seam | 4.0 | 1.3 | 3.63 | 13 | 1.2 | 0.2 |
| Huoluowan (22102 and 22104) | Muddy siltstone | 13.8 | 2.14 | 7.29 | 29.6 | 4.9 | 0.33 |
| | Medium quartz sand | 7.30 | 2.65 | 19.24 | 85.7 | 12.8 | 0.15 |
| | Muddy siltstone | 2.67 | 2.14 | 9.63 | 29.6 | 4.9 | 0.33 |
| | No. 2-2 upper seam | 2.70 | 1.35 | 2.13 | 13.4 | 1.23 | 0.29 |
| | Fine sandstone | 4.24 | 2.40 | 14.45 | 45.7 | 3.3 | 0.21 |
| | Quartz sandstone | 1.88 | 2.65 | 20.29 | 83.7 | 13 | 0.13 |
| | No. 2-2 seam | 2.50 | 1.35 | 2.24 | 13.4 | 1.23 | 0.29 |
| Zhangjiamao (15203) | Fine sandstone | 1.19 | 2.23 | 15.89 | 51.7 | 1.56 | 0.35 |
| | Siltstone | 1.91 | 2.42 | 9.24 | 43.8 | 1.25 | 0.27 |
| | Fine sandstone | 1.67 | 2.21 | 14.33 | 48.5 | 1.56 | 0.35 |
| | Mudstone | 1.78 | 2.50 | 6.13 | 6.29 | 0.28 | 0.19 |
| | Fine sandstone | 2.6 | 2.21 | 14.45 | 32.3 | 1.56 | 0.34 |
| | Mudstone | 2.8 | 2.48 | 6.29 | 6.30 | 0.28 | 0.19 |
| | No. 5-2 seam | 6.1 | 1.32 | 3.45 | 12.8 | 1.35 | 0.26 |
| Ningtiaota (N1114 and N1206) | Siltstone | 6.7 | 2.42 | 12.05 | 35.3 | 0.65 | 0.32 |
| | Medium sandstone | 9.96 | 2.33 | 19.49 | 40.6 | 1.5 | 0.28 |
| | No.1-2 seam | 1.89 | 1.29 | 4.25 | 15.7 | 1.3 | 0.28 |
| | Fine sandstone | 2.85 | 2.23 | 9.53 | 25.6 | 1.2 | 0.27 |
| | Fine sandstone | 6.55 | 2.27 | 12.58 | 29.6 | 1.5 | 0.29 |
| | Siltstone | 3.8 | 2.44 | 11.22 | 46.0 | 0.9 | 0.30 |
| | Fine sandstone | 5.90 | 2.34 | 16.29 | 48.5 | 1.9 | 0.27 |
| | Siltstone | 1.0 | 2.40 | 11.24 | 45.3 | 1.2 | 0.30 |
| | Fine sandstone | 11 | 2.60 | 16.63 | 43.6 | 1.5 | 0.35 |
| | Fine sandstone | 2.16 | 2.30 | 16.63 | 45.6 | 2.2 | 0.27 |
| | No. 2-2 seam | 4.60 | 1.34 | 4.45 | 13.8 | 1.4 | 0.27 |

### *2.2. Methods*

The physical similarity simulation experiment is convenient for people to intuitively acquaint and understand mining activities, and master the breaking law of mining on overlying strata. The main process is as follows.

First, the object of the physical simulation experiment is the prototype on site. According to the similarity theory, to satisfy the basic similar conditions (for example, geometric similarity, dynamic similarity and boundary similarity, etc.) in the simulation experiment body (for example: two/three-dimensional plane stress model frame, wind tunnels, sinks, etc.) to conduct the experiment to research the laws of the prototype [1,2]. Therefore, it is important to determine the geometric similarity ratio and select the appropriate model framework.

Second, based on the lithology in Table 1, the proportion of similar materials of each rock layer is determined, and the physical similar simulation experiment is laid forward. Generally, the aggregate selected from the rock layer is river sand, and the cementing material is gypsum and white powder. Impermeable clay or read clay was used to simulate the LSL and experimental oil was added to increase the viscosity. Then, we begin carrying out experimental excavation. All the experiments are excavated from left to right. In the process of mining, the total station and dial indicator are used to monitor the subsidence of overburden and surface. At the same time, select the appropriate fixed position. Use the high-definition camera to record the key experimental phenomena (Figure 2).


(**a**) (**b**) (**c**)

**Figure 2.** Monitor systems in physical simulation: (**a**) total station, (**b**) dial indicator, and (**c**) camera.

Lastly, the data of the experimental process is analyzed and processed. The innovations in this experimental process are using the experimental photos taken by a high-definition camera taken at the same location, using AutoCAD software to sketch the experimental process.

This paper is based on the physical simulation experiment to investigate the crack development characteristics in shallow coal seam mining. Two aspects need to be explained.

(1) The author focuses on the macroscopic crack development characteristics after the rock is mined and destroyed in this paper. There are some limitations in the existing experimental conditions and methods. It is impossible to simulate the micro-cracks, voids, and other structures inside the rock mass. In addition, the behavior before and after the rock mass destruction is very complicated. Therefore, macro cracks and microstructures are not involved in this paper.

(2) Table 1 shows the types of overburden mentioned are bedrock layer, red soil layer, sandy layer, and quicksand layer. According to the orthogonal experimental method, the authors made standard test pieces for different proportions, and carried out experiments on uniaxial compressive strength in the laboratory. Based on the geometric similarity ratio, the intensity similarity ratio is determined, the result is obtained by the conversion of the intensity similarity ratio, which is compared with the strength of the corresponding layer of the prototype. The closest matching ratio number is selected to simulate the paving of each rock layer on the working surface to reduce the source of error in the experiment. With a large number of experiments, the authors used different aggregates and ratios to simulate the mechanical and structural characteristics of elastoplastic deformation or viscoelastic deformation characteristics of the rock (for example, red soil layer and the sand layer), and all of them achieved good experimental results.

## 3. Evolution Law of Cracks in Shallow Coal Seam

### 3.1. PSCEL of Typical Shallow Coal Seam

Taking the 1203 working face of Daliuta Coal Mine as the background, the No. 1-2 seam mines 68 m deep, the thickness of bedrock is 19 m and LSL is 45 m, and the mining height is 4.0 m. The geometric ratio is 1:100. When the face has advanced to 32 m, the roof caves for the first time, the thick LSL showed "loose arch" damage (Figure 3, black line) when advanced to 48 m. During the first periodical weighting, the LSL was still "arch" and the crack development height was 26 m (Figure 3, red line). When advanced to 64 m, the second periodical weighting, the "arch shell"-like separation zone is formed in the thick LSL (Figure 3, blue line). After reaching a full mining stage, the surface is generated in front of the coal wall. A physical simulation sketch of a typical shallow coal seam mining is shown in Figure 3. The sketch map of simulation is to sketch the fixed-point photographs in the simulation experiment frame one-by-one in sequence. Each color represents the crack of working face periodically falling at different times.

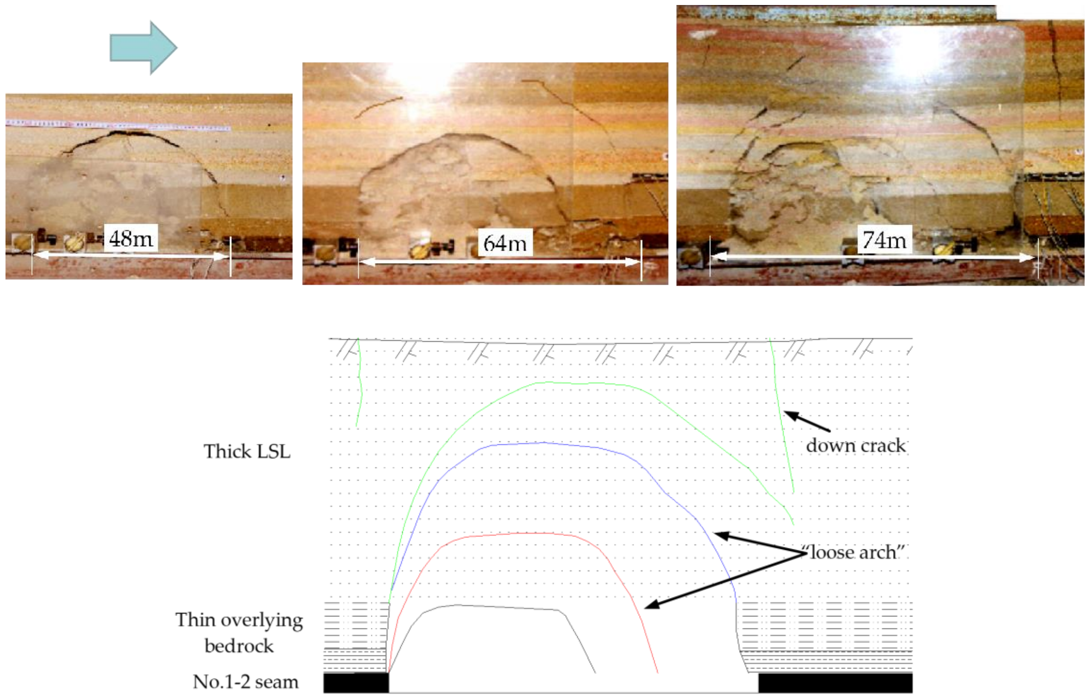


**Figure 3.** Sketch drawing of evolution of periodic cracks in mining.

According to Figure 3, we found the cracks include upward cracks that develop from the bottom to the top, and down cracks develop from the top to the bottom. The upward cracks have SEC and DPC in the face, and the downward cracks have tensile cracks in the surface LSL or bedrock.

In the typical shallow coal seam mining process, the SEC increases with the face advanced distance. The roof breaking angle is about 65°. After full mining, the periodic segmentation of the roof plate shows the phenomenon of "secondary arching" in the curved rock pillars on the two broken rock blocks, and the surface steps sink down (Figure 4).

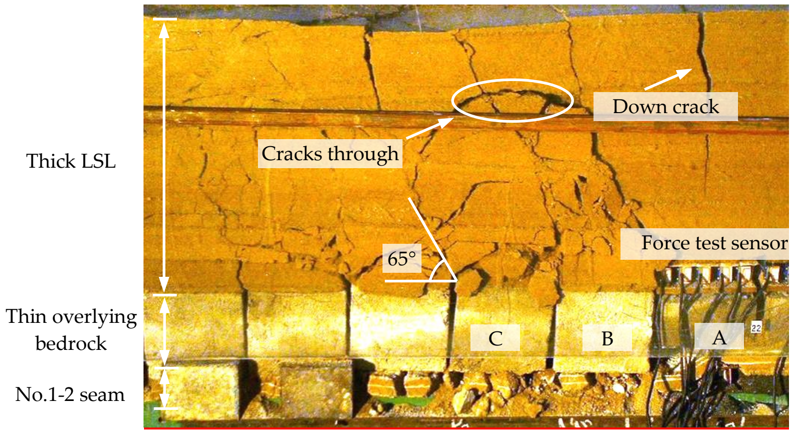


**Figure 4.** Periodic arc-shaped pillars and arching.

In addition, Figure 4 shows the periodic cracks of the overlying strata in the thick LSL are periodically "arc rock pillars" and the height of the arc develops rapidly with the increase of the face advancing distance.

Figure 5 shows the critical value of the A key block support pressure is continuously reduced. The average load of the thick LSL on the B key block is reduced and the key block of C is not changed much, which indicates that the caving of thick LSL requires a certain time and process in the gob.

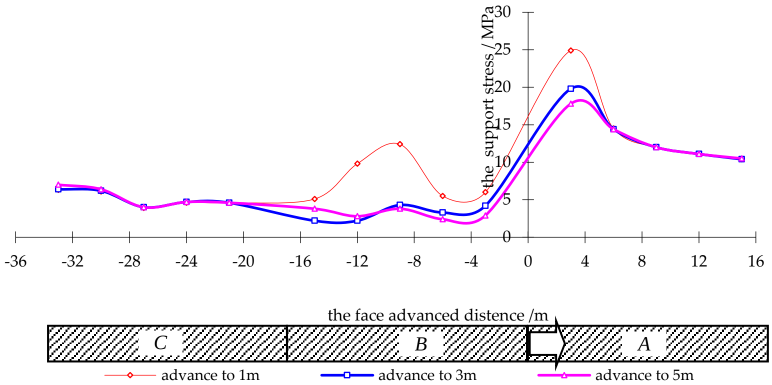


**Figure 5.** Key block dynamic load change in mining.

## 3.2. *PSCEL of Nearly Shallow Coal Seam*

Taking 22102 working face of Huoluowan Coal Mine as the background, the face is located in No. 2-2 upper seam, the seam buried depth is 115 m, the thickness of LSL is 27 m, and the thickness of overlying bedrock is 88 m, the mining height is 2.5 m, and the similarity ratio is 1:100.

The development of the overlying cracks in the experimental process of 22102 working face is sketched (Figure 6). The DPC in the subsidence basin are closed in the affected layer of the overburden structure, the surface settlement is slowed down, and the stratum presents a certain self-repair. During the process of advancing the working face, the overburden is still moving in the gob. The original separation or cracks has decreased or closed with the movement of the overburden. It could account for the stratum presenting self-repair characteristics.

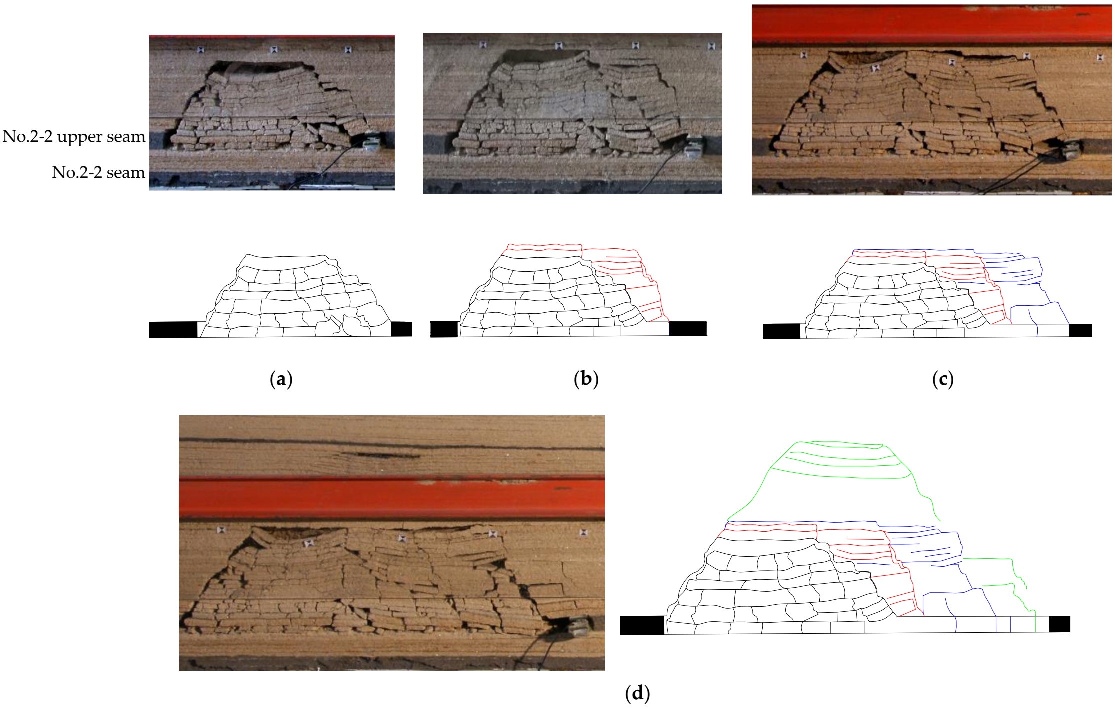


**Figure 6.** Crack development in different positions of 22102 working face: (**a**) advanced to 60 m, (**b**) advanced to 67.5 m, and (**c**) advanced to 80 m, and (**d**) advanced to 90 m.

*3.3. PSCEL of Large Mining Height Cracks in Shallow Coal Seam*

Under the large mining height face, the development height and width of the crack (including SEC and DPC) have a relationship with the mining height. Taking 15201 working face of Zhangjiamao Coal Mine as the background, the average buried depth is 120 m, the thickness of LSL is 50 m, the thickness of bedrock is 70 m, the mining height is 6.2 m, and the geometric ratio is 1:50.

Using the principle of controlling single variables in the physical simulation, the method of variable height of the slabs simulates the regularity of mining PDC under the mining height, which is 4 m, 5 m, and 6 m on the same model (Figure 7).

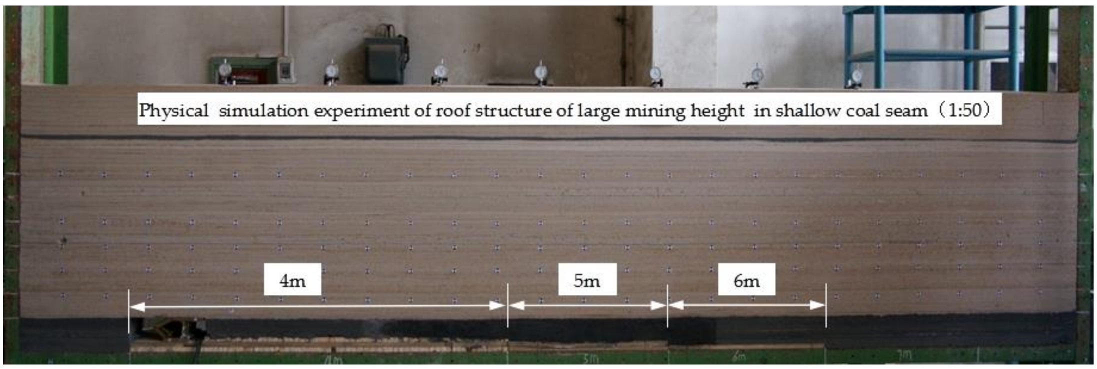


(**a**)

**Figure 7.** *Cont.*

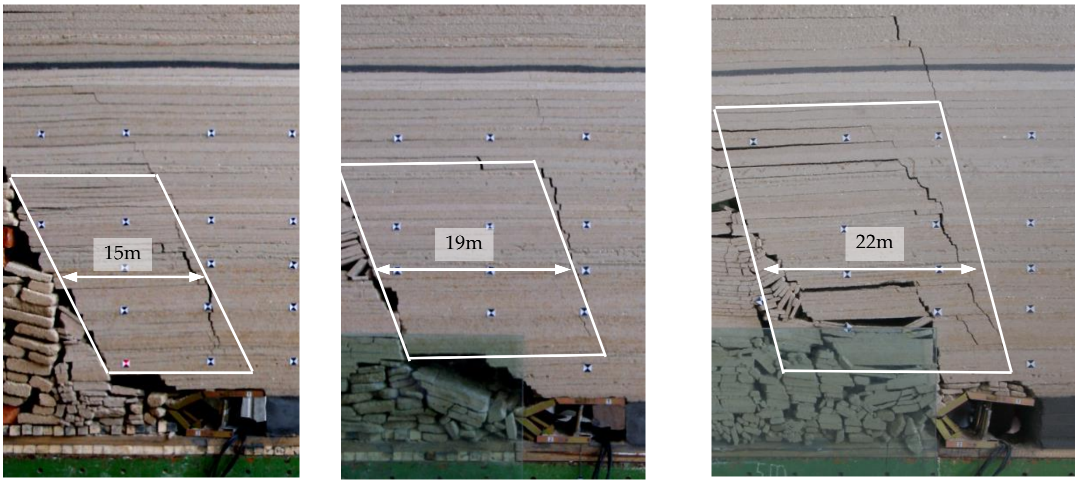


(**b**) (**c**) (**d**)

**Figure 7.** Simulated the mining height at 4 m, 5 m, and 6 m: (**a**) physical simulation model, (**b**) the mining height is 4 m, (**c**) the mining height is 5 m, and (**d**) the mining height is 6 m.

Figures 7 and 8 show the DPC evolution under different mining heights. The height is the only variable. As the mining height increases, the periodical weighting intervals and the range of cracks and the crack development speed grow.

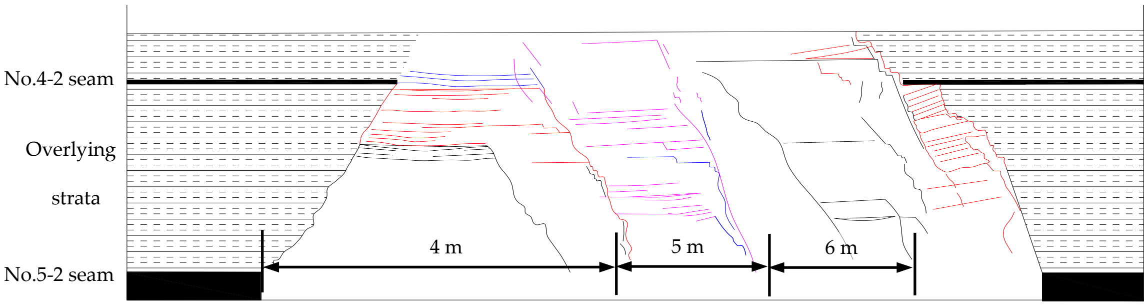


**Figure 8.** Sketch drawing of the dynamic periodic crack evolution under different mining heights.

In the actual mining process, the ground surface crack development law is observed manually. In the initial mining stage of the 6 m large mining height working face and the step type sinks. The surface damage is extremely serious. Figure 9 shows the surface damage from the step cracks in the shallow coal seam mining. The coal mine ecological resources are threatened.

(**a**) (**b**)

**Figure 9.** Surface damage from the step cracks: (**a**) step crack, and (**b**) the height of step crack is 1.6 m.

## 4. Evolution Laws of Cracks in Multiple-Seam Mining

Through the physical simulation analysis of typical shallow coal seam and near shallow coal seam, it was concluded that different types of shallow coal seam mining have different development characteristics for SEC and DPC. In a typical shallow coal seam, the development of SEC are dominated, which leads to the failure of the LSL-like arch. However, the development of SEC is dominated by parabolic failure of rock layers in a nearly shallow coal seam.

### *4.1. PSCEL of Shallow Utmost Closely Spaced Multiple-Seam*

Taking 22104 working face of Huoluowan Coal Mine as the engineering background, the face buried depth of 125 m and a mining height of 2.5 m is located in 2-2 coal seam and close to the upper coal seam gob of 5 to 7 m.

When the 22104 working face has advanced to 20 m, the inter-burden strata completely broke, which leads to the gob of the upper and lower working face is connected (Figure 10a). The broken roof caves massively for the first time and the activated crack height is 20 m. When the face advanced to 27.5 m, the height of the activated crack is 29 m, and the crack of the upper seam is widened (Figure 10b). When the face advanced to 35 m, the height of the activated crack reaches 34 m (Figure 10c).

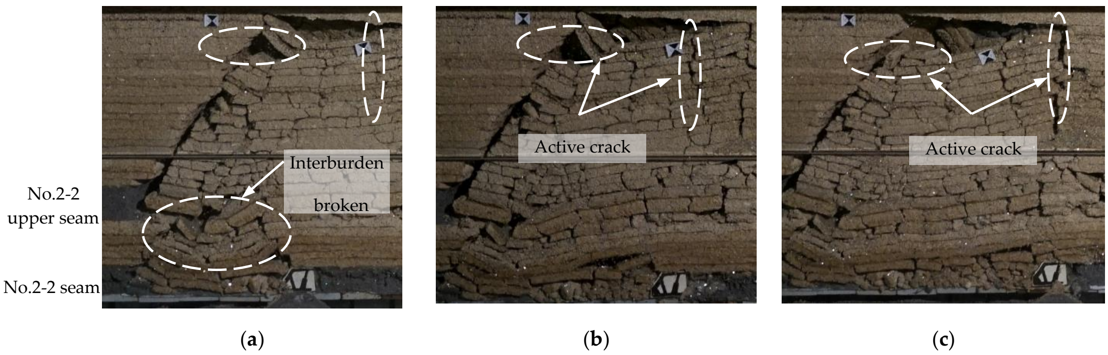


**Figure 10.** 22104 working face activation cracks development schematic diagram: (**a**) advanced to 20 m, (**b**) advanced to 27.5 m, and (**c**) advanced to 35 m.

As the face has advanced 38 to 58 m, the periodical weighting of the broken roof is about 5 to 7.5 m, the crack development speed of the overburden is significantly increased, and the average load of the simulated support is 7150 kN/frame. When the face has advanced 58 to 78 m, the crack development is not clear and the average load of the simulated support is 4810 kN/frame. The development speed and range of the activation crack lead to the "High Pressure Zone" (HPZ) and "Low Pressure Zone" (LPZ) as shown in Figure 11. According to Figure 11, when the lower seam roof caves height's slope increased more than the upper seam in multi-seam mining, it will cause the face HPZ phenomena.

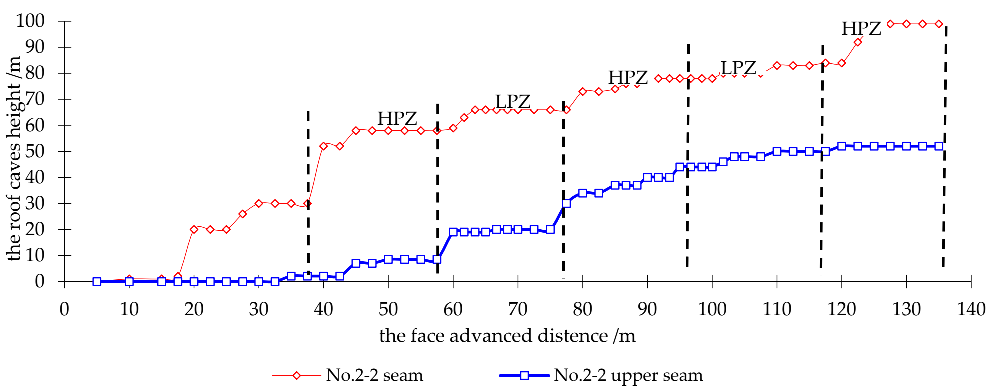


**Figure 11.** Advanced to 40 ~ 65 m high-pressure zone of the cracks activation.

When the mining reaches ultra-sufficient mining, the activation cracks in the overburden are developed, as shown in Figure 12. The SEC has developed on the surface, which forms the step crack shapes. The crack at the surface of the upper coal seam is reactivated, and the depth and width of the crack is increased.

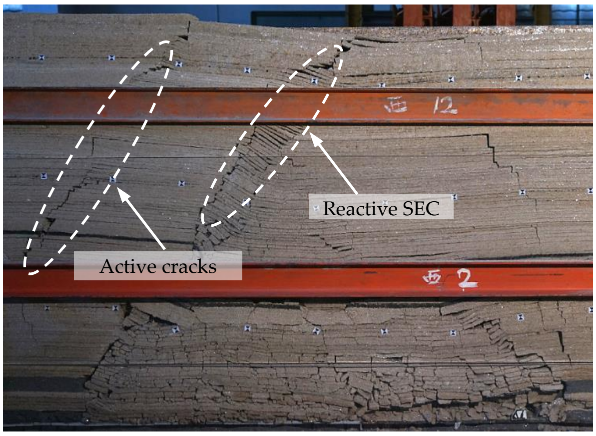


**Figure 12.** Development of cracks in overlying strata after supercritical mining.

The sketches of the crack activation and development process of the 22104 working face when entering and crossing the coal pillar are selected (Figure 13) and the width of the upper pillar is 25 m. Four colors represent four locations in the face. The black represents Figure 13a, the red represents Figure 13b, the blue represents Figure 13c, the green represents Figure 13d, and the physical simulation in different position's schematic diagram are shown in Figure 13e–g.

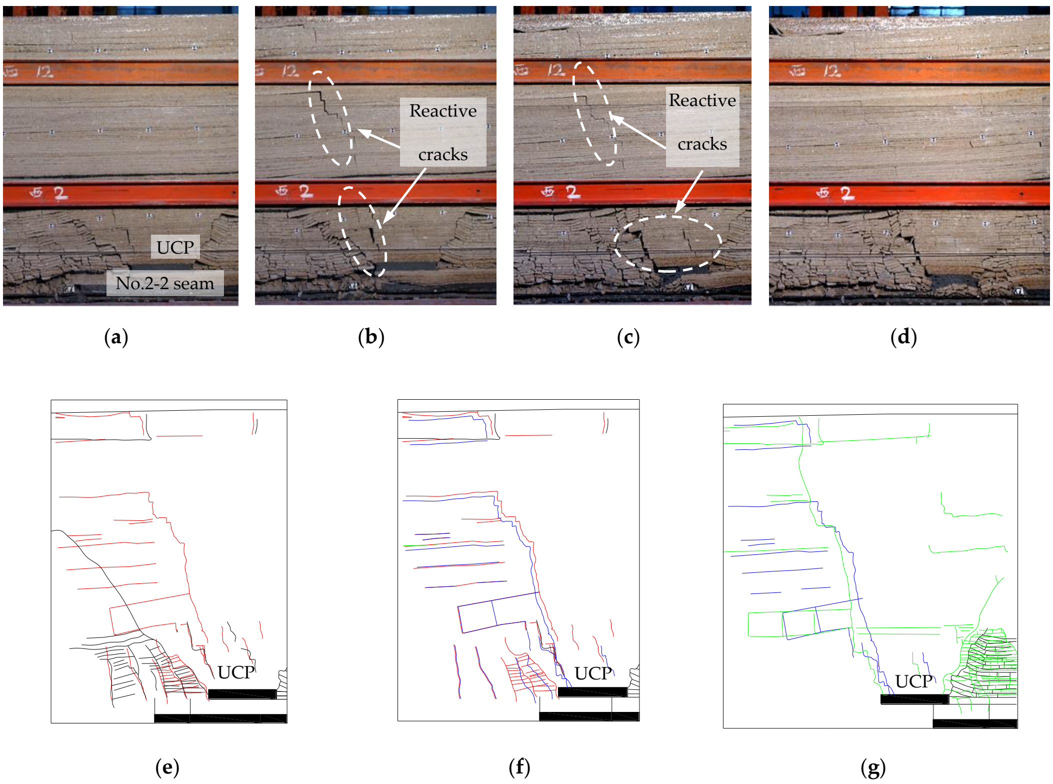


**Figure 13.** CPC activation schematic diagram: (**a**) 20 m from the UCP left side, (**b**) 10 m from the UCP left side, (**c**) before 10 m from the UCP right side, (**d**) behind 20 m from the UCP right side, (**e**) comparative positions (**a**,**b**), (**f**) comparative positions (**b**,**c**), (**g**) comparative positions (**c**,**d**).

Figure 13e illustrates that the working face has advanced Figure 13a,b, the face entering the upper coal pillar (UCP) inverted trapezoidal affected zone, with the range and height of the coal pillar cracks (CPC) increasing. Compared with Figure 13b,c, the range and height of CPC grows insignificantly. However, the UCP inverted trapezoidal affected zone caved massively, while the face advanced after the UCP, as shown in Figure 13g. Combined with the production practice, the working face will occur in the midst of mine pressure in crossing the range of UCP.

### 4.2. PSCEL of Shallow Closely Spaced Multiple-Seam

The N1114 working face in No.1-2 coal seam (upper seam) and the N1206 working face in No. 2-2 coal seam (lower seam) of the Ningtiaota Coal Mine. The N1114 working face buried depth is 123 m, the thickness of bedrock is 81 m, the thickness of LSL is 42 m, and the height of mining is 1.75 m. The N1206 working face buried depth is 163 m, the thickness of bedrock is 121 m, the thickness of LSL is 42 m, the mining height is 5.46 m, and the geometric ratio is 1:200.

Since the N1114 working face has advanced to 55 m, during the main roof first weighting, the crack height was 18 m. When the face advanced to 74 m, the main roof first periodic weighting and the crack height was 26 m. As the face advanced to 97 m, the height of the crack was 43 m. When the face advanced to 110 m, the height of the crack was 46 m (Figure 14).

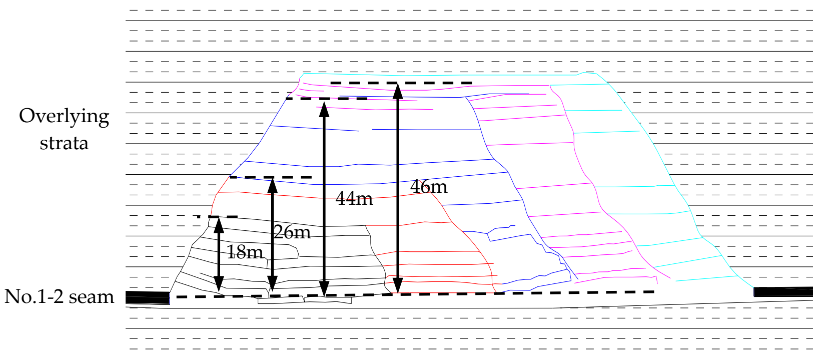


**Figure 14.** Sketch drawing of evolution of DPC in N1114 working face mining.

The No.1-2 seam was excavated in the model. The seam included the N1114 working face and the N1115 working face, their width is 245 m and the coal pillar is 20 m. The "W" type surface subsidence line is shown in Figure 15. When the working face of the lower seam has advanced to the range of the section coal pillar by the upper seam, due to the influence of the section coal pillar the surface subsidence value is smaller than other locations.

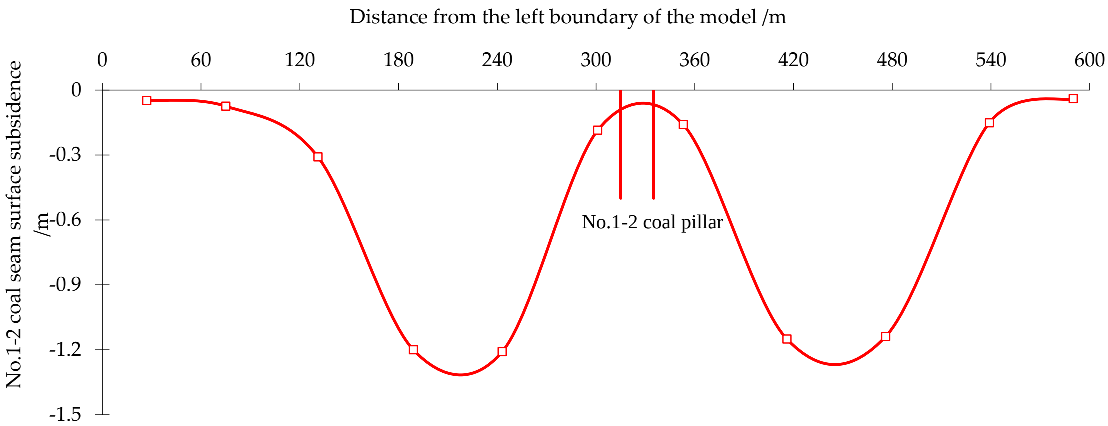


**Figure 15.** Surface "W-shape" subsidence curve after 1-2 coal seam physical simulation mining.

Figure 16 shows the DPC activation of the schematic diagram in the face advanced in different locations. The black lines represents the first weighting. The DPC height is 29 m. The red lines represent the first periodic weighting. The DPC height is 56 m with inter-burden bedrock completely broken, and the activated upper and lower gobs are through. The blue lines represent the second periodic weighting. The activated crack height is 94 m. When the face has advanced to 130 m, the green lines represent the fourth periodic weighting and the activated crack height reaches 163 m.

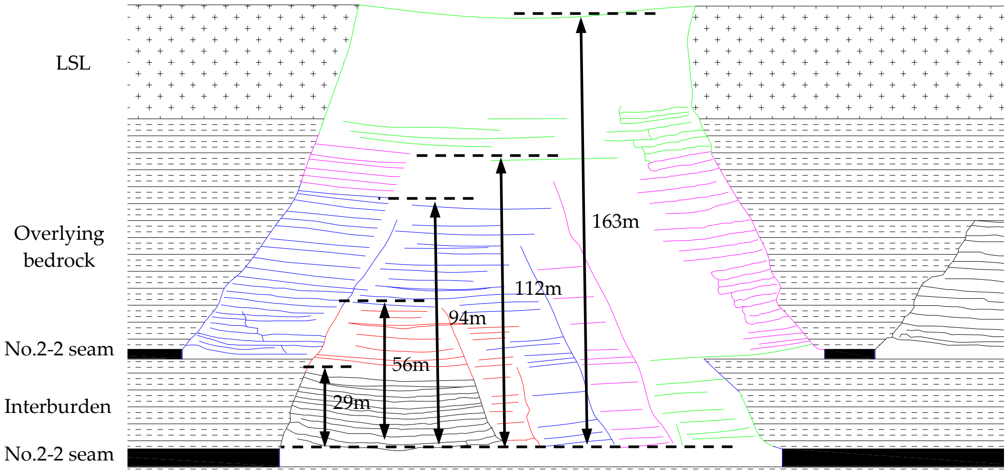


**Figure 16.** N1206 working face DPC activation development schematic diagram.

Combined with field measurement, when the upper seam working face has mined finished, the fixed crack was selected for observation in the overlapping area of the N1114 and N1206 working faces, as shown in Figure 17a. With the mining of the lower seam, when the working face has advanced to the fixed crack location, the crack width increased (Figure 17b,c).

(a) (b) (c)

**Figure 17.** Field measurement of DPC: (**a**) the upper seam working face has mined finished, (**b**) the lower seam working face has finished with the same location, and (**c**) the lower seam working face has advanced through the position of DPC.

When the face enters and across the UPC (Figure 18), the CPC is gradually activated before the coal pillar enters the coal pillar, the width of the coal pillar crack increases, and the surface subsidence increases. After the coal pillar, the "inverted trapezoid" body structure of the pillar is completely sunk, the activated CPC are closed again, and the surface subsidence is reduced.

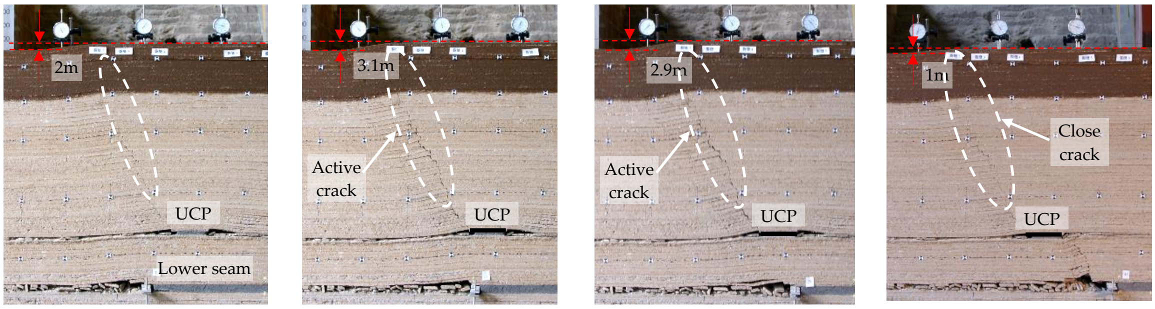


(a) (b) (c) (d)

**Figure 18.** Distance from the center UCP: (**a**) 10 m, (**b**) aligned pillar, (**c**) 0 m, and (**d**) 40 m.

When the 2-2 seam (lower seam) has mined, compared with the surface subsidence value of the 1-2 seam (upper seam), as shown in Figure 19. Figure 19 shows the coal pillars can effectively reduce surface subsidence, for example, the corresponding surface subsidence value of the No.2-2 coal pillar is 2.59m and the No.1-2 coal pillar is 2.84m, however, the maximum value of surface subsidence is 4m. Separately reduced 1.41m and 1.16m.

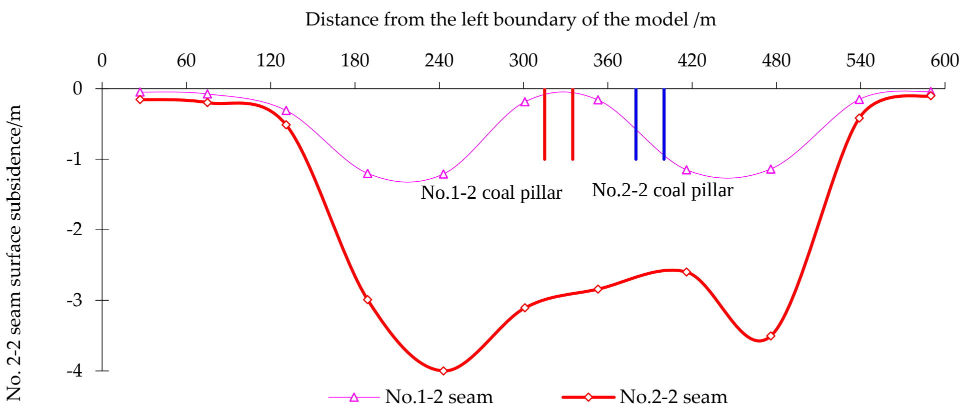


**Figure 19.** Surface subsidence of 2-2 seam from the physical simulation mining.

## 5. Effect of Coal Pillar Group Structure in Multiple-Seam Mining

The coal pillar is ensuring the stability of the roadway during the mining process in the lower seam while the stability of the coal pillar mainly affects the stability of the upper seam gob. However, in multiple-seam mining, the size, location, and stability of the coal pillars have a direct impact on the layout of the lower coal seam face.

Figure 20 shows the reasonable coal pillars spacing in the multiple-seam mining and can reduce the surface uneven subsidence. Based on the physical simulation of the Ningtiaota coalmine, when the 2-2 coal pillar is separated from the 1-2 coal pillar by 40 m, and the 3-1 coal pillar is separated from the 2-2 coal pillar by 80 m, the surface sinks evenly.

Table 2 and Figure 21 present the position of the coal pillar, which corresponds to the minimum value of the absolute subsidence value, and the subsidence of the affected area of the coal pillar "inverted trapezoid" slows. The absolute subsidence value of the surface are roughly equal, and the rational self-repair of the overlying strata can be achieved through reasonable coal pillar spacing.

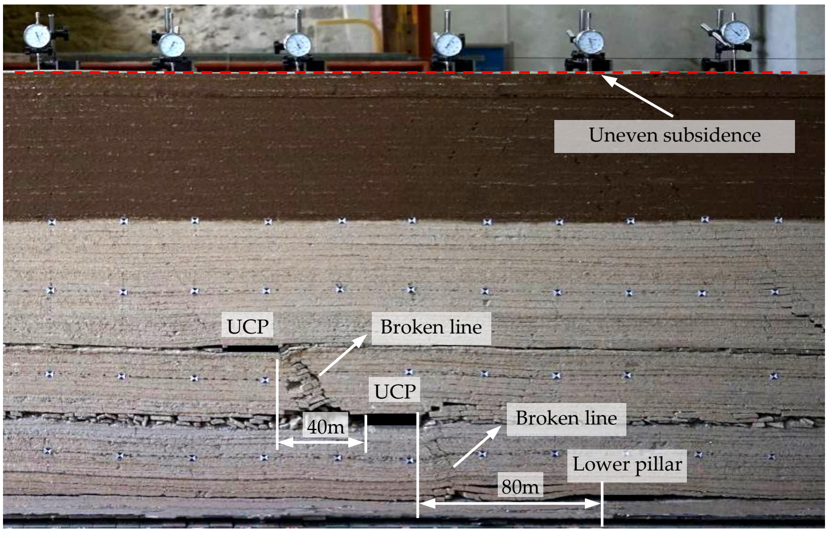


**Figure 20.** Surface subsidence uniformly with reasonable coal pillars.

**Table 2.** Absolute subsidence value and factor in coal pillars position after multiple-seam mining.

| | Coal Seam | No.1-2 Coal Pillar | No.2-2 Coal Pillar | No.3-1 Coal Pillar |
|---|---|---|---|---|
| Absolute Subsidence Value/m | No.1-2 seam | 0.18 | 1.20 | 1.21 |
| | No.2-2 seam | 2.98 | 1.85 | 2.79 |
| | No.3-1 seam | 2.05 | 2.18 | 1.49 |
| | Total | 5.21 | 5.23 | 5.29 |
| Absolute Subsidence Factor/% | No.1-2 seam | 0.06 | 0.64 | 0.64 |
| | No.2-2 seam | 0.65 | 0.40 | 0.60 |
| | No.3-1 seam | 0.75 | 0.80 | 0.54 |

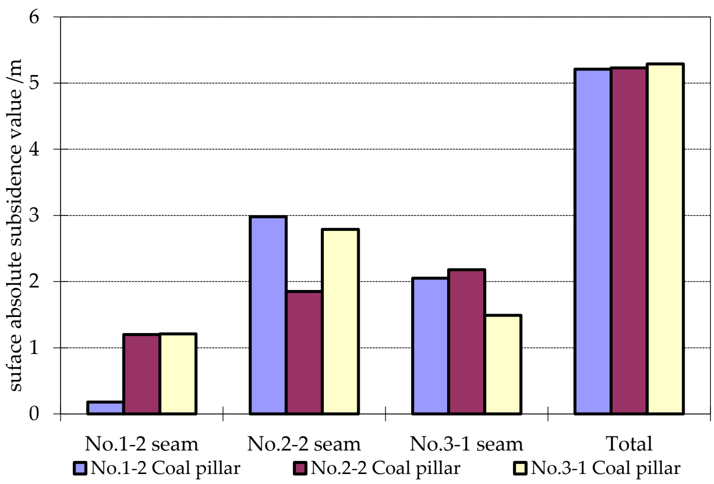


**Figure 21.** Absolute subsidence value in coal pillars position after multiple-seam mining.

According to "Deformation Monitoring and Subsidence Engineering" [25], the length and width of the gob reach and exceed 1.2$H$~1.4$H$ ($H$ is buried depth) is the sufficient condition for critical mining. When the shallow multiple-seam mining in the Shenfu coalfield, the face has reached supercritical mining. The remaining coal pillars are the main reason of an uneven surface settlement. The author believes that the reasonable coal pillar spacing is arranged by the "inverted trapezoidal" structure formed by the UCP in the uneven settlement area, combined with the distribution range of the coal pillars in the floor stress, with the structural effect of the coal pillar group, and the width of the surface crack, the drop gradually decreases or closes and the surface subsidence basin increases. This realizes the self-repair of the ecological environment in the mining area and achieves the goal of green mining.

## 6. Conclusions

Through physical simulation and measurement, the SEC development is dominated by sand-arched failure, and the surface crack is almost directly above the setup entry in typical shallow coal seam mining. However, in near shallow coal seam mining, the SEC development is dominated by parabolic damage, and the surface crack is located inside the setup entry. As the mining height increases, the crack growth rate and extent of damage increase significantly.

The overlying bedrock cracks in shallow coal seam mining are divided into two types: upward crack and downward crack, according to the development direction. According to the development position, they are divided into three kinds: SEC, DPC, and boundary crack. The temporary DPC generation and closure shows the ability of the formation to self-repair. The permanent fixed crack is the main object to be controlled in a production practice. However, the quantitative analysis of the development of activated cracks needs further improvement during the repeated mining of shallow multiple-seam.

The coal pillar of the multiple-seam is the main reason for the uneven settlement of the surface. Through reasonable coal pillars spacing, the relatively uniform settlement of the surface and the overlying bedrock cracks can be controlled. The self-repair and green mining of the ecological environment in the mining area can be realized.

**Author Contributions:** Conceptualization, Q.H. Experimental Design, Q.H., Y.H. and J.C. Validation, Q.H. and Y.H. Theoretical Analysis, Q.H. and Y.H. Data Curation, Y.H. and J.C. Supervision, Q.H. Writing—Original Draft Preparation, Y.H. Writing—Review & Editing, Q.H. and Y.H. Supervision, Q.H. Project Administration, Q.H. Funding Acquisition, Q.H.

**Funding:** The National Natural Science Foundation of China, grant number No.51674190, funded this research.

**Acknowledgments:** We thank the National Natural Science Foundation of China for its support of this study. We thank the academic editors and anonymous reviewers for their kind suggestions and valuable comments.

**Conflicts of Interest:** The authors declare no conflict of interest.

## References

1. Huang, Q.X. *Study on Roof Structure and Ground Control in Shallow Seam Longwall Mining*; China University of Mining and Technology Press: Xuzhou, China, 2000.
2. Wang, S.M.; Huang, Q.X.; Fan, L.M.; Wang, W.K. *The Key Technology of Water Conservation Mining in Fragile Ecologically Mining Coal Resources*; Science Press: Beijing, China, 2010.
3. Qian, M.G.; Miao, X.X.; Xu, J.L.; Cao, S.G. On Scientized Mining. *J. Min. Saf. Eng.* **2008**, *25*, 1–10.
4. Qian, M.G.; Xu, J.L.; Wang, J.C. Further on the sustainable mining of coal. *J. China Coal Soc.* **2018**, *43*, 1–13.
5. Huang, Q.X.; Zhang, P. Study on dynamic load distribution on key roof blocks of under thick sandy soil stratum. *Chin. J. Rock Mech. Eng.* **2004**, *23*, 4179–4182.
6. Huang, Q.X. Study on loading distribution law on key roof and its structure upon mining face under thick sandy layer. *J. China Univ. Min. Technol.* **2005**, *34*, 289–293.
7. Huang, Q.X. Research on roof control of water conservation mining in shallow seam. *J. Min. Saf. Eng.* **2017**, *42*, 50–55.
8. Huang, Q.X.; Zhang, W.Z. Mechanical model of water resisting strata group in shallow seam strip-filling mining. *J. China Coal Soc.* **2015**, *40*, 973–978.
9. Liu, H.; He, C.G.; Deng, K.Z.; Bian, Z.F.; Fan, H.D.; Lei, S.G.; Zhang, A.B. Analysis of forming mechanism of collapsing ground fissure caused by mining. *J. Min. Saf. Eng.* **2013**, *30*, 380–384.
10. Liu, H.; Deng, K.Z.; Lei, S.G.; Bian, Z.F.; Chen, D.Y. Dynamic developing law and governance standard of ground fissures caused by underground mining. *J. Min. Saf. Eng.* **2017**, *34*, 884–890.
11. Hu, Z.Q.; Wang, X.J.; He, A.M. Distribution characteristic and development rules of ground fissures due to coal mining in windy and sandy region. *J. China Coal Soc.* **2014**, *39*, 11–18.

12. Hu, Z.Q.; Long, J.H.; Wang, X.J. Self-healing natural restoration and artificial restoration of ecological environment for coal mining. *J. China Coal Soc.* **2014**, *39*, 1751–1757.
13. Fan, L.M.; Zhang, X.T.; Xiang, M.X.; Zhang, H.Q.; Shen, T. Characteristics of ground fissure development in high intensity mining area of shallow seam in Yushenfu coal field. *J. China Coal Soc.* **2015**, *40*, 1442–1447.
14. Fan, L.M.; Ma, X.D.; Li, Y.H.; Li, C.; Yao, C.W. Geological disasters and control technology in high intensity mining area of western China. *J. China Coal Soc.* **2017**, *42*, 276–285.
15. Chen, J.J.; Zhu, L.J.; Yan, W.T.; Wang, M.Y. Analysis on distribution characteristic and formation mechanism of surface fissures caused by high intensity mining. *J. Saf. Sci. Technol.* **2015**, *11*, 96–100.
16. Chen, J.J.; Zou, Y.F.; Guo, W.B. Study on the Relationship Between Subsidence Coefficient and Mining Degree Under A Thick Alluvium Stratum. *J. Min. Saf. Eng.* **2012**, *29*, 250–254.
17. Kang, J.R. Analysis of effect of fissures caused by underground mining on ground movement and deformation. *J. Rock. Mech. Eng.* **2008**, *27*, 59–64.
18. Fan, G.W.; Zhang, D.S.; Ma, L.Q. Overburden movement and fracture distribution induced by longwall mining of the shallow coal seam in the Shendong coalfield. *J. China Univ. Min. Technol.* **2011**, *40*, 196–201.
19. YU, X.Y.; Li, B.B.; Li, R.B.; Duan, W.S.; Liu, P.L. Analysis of mining damage in huge thick collapsible loess of western China. *J. China Univ. Min. Technol.* **2008**, *37*, 43–47.
20. Peng, J.B.; Chen, L.W.; Huang, Q.B.; Men, Y.M.; Fan, W.; Yan, J.K.; Li, K.; Ji, Y.S.; Shi, Y.L. Large-scale physical simulative experiment on ground-fissure expansion mechanism. *Chin. J. Geophys.* **2008**, *51*, 1826–1834.
21. Mao, S.J.; Yang, N.S.; Gao, Y.Q.; Zhang, P.P.; Wu, D.Z. Design and key technology research of coal mine distributed cooperative "one map" system. *J. China Coal Soc.* **2018**, *43*, 280–286.
22. Zhang, W.; Zhang, D.S.; Wu, L.X.; Wang, H.Z. On-site radon detection of mining-induced fractures from overlying strata to the surface: A case study of the Baoshan Coal Mine in China. *Energies* **2014**, *7*, 8483–8507. [CrossRef]
23. Xu, D.J.; Peng, S.P.; Xiang, S.Y.; He, Y.L. A novel caving model of overburden strata movement induced by coal mining. *Energies* **2017**, *10*, 476. [CrossRef]
24. Huang, Q.X. Ground pressure behavior and definition of shallow seams. *J. Rock Mech. Eng.* **2002**, *21*, 1174–1177.
25. Deng, K.Z.; Tan, Z.Q.; Jiang, Y.; Dai, H.Y.; Shi, Y.; Xu, L.J. *Deformation Monitoring and Subsidence Engineering*; China University of Mining and Technology Press: Xuzhou, China, 2014.


© 2019 by the authors. Licensee MDPI, Basel, Switzerland. This article is an open access article distributed under the terms and conditions of the Creative Commons Attribution (CC BY) license (http://creativecommons.org/licenses/by/4.0/).